今回の結果と直接比較することは困難であるが，我々の結果と同様にLVAの有効性を示したものと考えられる．

リンパ管静脈吻合の本数に関しては，我々は1肢に対し平均1.57本のリンパ管静脈吻合を行い，全例でGood以上の結果を得た．リンパ管静脈吻合を数多く行ったほうがよいとの報告[1)6)]もあるが，光嶋ら[5)]はリンパ液の漏出が良好なリンパ管を見出せば1本のリンパ管静脈吻合でも術後に著明な改善が得られたと報告している．今回ICG蛍光リンパ管造影法を用いる事により，まだリンパ管としての機能を残しているリンパ管を見つけ出し皮静脈に吻合できた事により良好な結果が得られたものと考えられる．

ま と め

1．男性下肢リンパ浮腫症例6例（7肢）に対しICG蛍光リンパ管造影法を用いたLVAを施行し，6ヵ月以上の経過観察を行った．

2．結果はExcellent 4肢，Good 3肢，Fair 0肢，Poor 0肢であった．

3．リンパ管静脈吻合術において，ICG蛍光リンパ管造影法を用いることにより，リンパ管の同定が容易となり，静脈との吻合がより確実になった．

文 献

1）Huang, G.K.：Microlymphaticovenous anastomosis for treating lymphedema. J. J.p.n. Soc. Plast. Reconstr. Surg., 7：905—911, 1987.

2）Koshima I., Inagawa K., Urushihara K., et al.：Supermicrosurgical lymphaticovenular anastomosis for the treatment of lymphedema in the upper extremities. J. Reconstr. Microsurg., 16：437—442, 2000.

3）Koshima I., Nanba Y., Tsutsui T., et al.：Long-term follow-up after lymphaticovenular anastomosis for lymphedema in the leg. J. Reconstr. Microsurg., 19：209—215, 2003.

4）Koshima I., Nanba Y., Tsutsui T., et al.：Minimal invasive lymphaticovenular anastomosis under local anesthesia for leg lymphedema. Annals of Plastic Surgery, 53：261—266, 2004.

5）光嶋 勲，森口隆彦，梶原康正：リンパ浮腫の治療．手術，50：1715—1723, 1996.

6）寺田 康，井島 宏，堀原 一：リンパ浮腫に対するリンパ管静脈吻合術．外科，50：165—168, 1988.

7）照喜納光信，高見昌司，諸岡久香，他：ICG蛍光リンパ管造影法を用いたリンパ管静脈吻合術．第49回日本形成外科学会総会・学術集会抄録集，：191, 2006.

日手会誌（J Jpn Soc Surg Hand），第25巻　第5号　659-662，2009

自由投稿論文

ICG蛍光リンパ管造影法を用いた上肢リンパ浮腫に対するリンパ管静脈吻合術

長谷川健二郎，渡邉敏之，杉山成史，徳山英二郎，木股敬裕

Key words : lymphedema（リンパ浮腫），lymphaticovenous anastomosi（リンパ管静脈吻合術），microsurgery（マイクロサージャリー），supermicrosurgery（超微小血管吻合術），fluorescence lymphography（蛍光リンパ管造影法）

【緒　言】

上肢リンパ浮腫に対するリンパ管静脈吻合術（LVA: lymphaticovenous anastomosis）において，インドシアニングリーン（ICG）蛍光リンパ管造影法（FL-ICG：fluorescence lymphography using ICG）を用いることにより，リンパ管の同定，静脈との吻合がより確実になったので，その有用性について報告する．

【対象と方法】

対象は2006年4月にICG蛍光リンパ管造影法を導入した後にLVAを施行し，術後5ヶ月以上の経過観察が可能であった上肢リンパ浮腫12症例12肢である．

方法はまず手背，手関節掌側，前腕部にICGを皮内注射し，特殊な赤外線カメラ（Photo Dynamic Eye：PDE　浜松ホトニクス社製）にて観察した（図1-A）．このカメラは皮下約2cmの深さまでICGの流れを観察することが可能で，ICGがリンパ管へ取り込まれ，リンパ流に乗り広がっていくのが観察出来る（図1-B）．リンパ管はICGの線状の流れとして観察され，同部を切開し顕微鏡下にリンパ管を探して確認し，皮静脈と吻合した（図1-C）．吻合直後にPDEで観察すると，吻合に問題がなければリンパ管からリンパ液が静脈内に流入するのが確認できた（図1-D）．評価は図2の如く，上肢の5ヶ所で周囲径を測定し，術前の周囲径に対する術後の周囲径の割合（改善率）をもとめ，いずれかの部位で89%以下に改善したものをExcellent（図3-A），90~95%の改善をGood（図3-B）とした．96~104%の変化は測定誤差を考慮し不変と考えFair（図3-C）とした．そしていずれの部位にも改善を

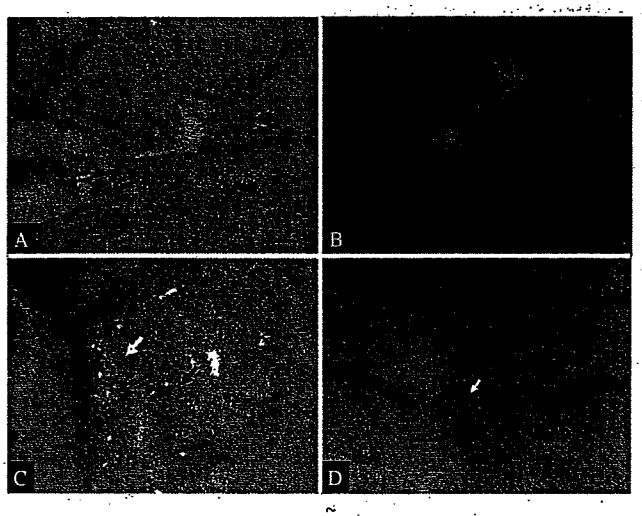

図1：ICG蛍光リンパ管造影法を用いたLVA
A：ICGを第2指間で皮内注射し，PDEで　　観察
B：造影された手背のリンパ管をボールペンでマーキング
C：LVA終了時（白色矢印：皮静脈，黒色矢印：リンパ管）
D：PDEによるLVA直後の観察（白色矢印：造影された皮静脈，黒色矢印：造影されたリンパ管）

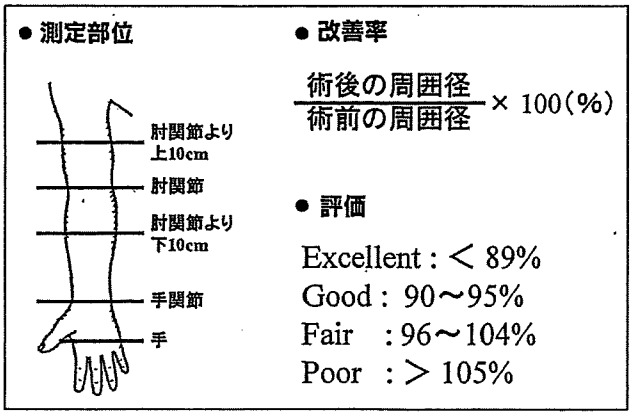

図2：評価方法

岡山大学医学部形成再建外科　〒700-8558　岡山県岡山市鹿田町2-5-1
Address for reprints : Kenjiro Hasegawa, Department of Plastic and Reconstructive Surgery, Okayma University Graduate School of Medicine and Dentistry, 2-5-1 Shikata, Okayama City 700-8558, Japan

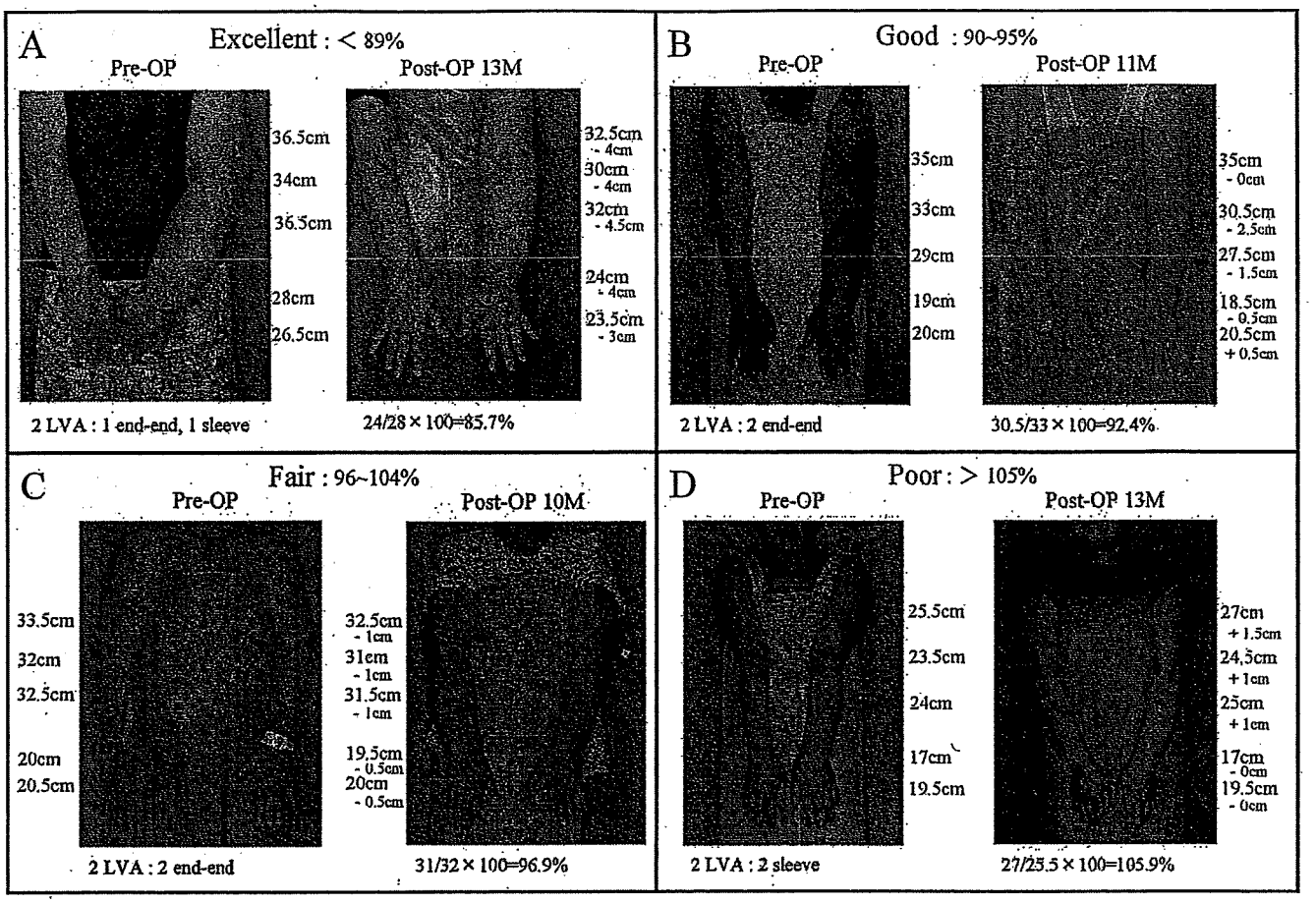

図3：評価に基づく代表症例
A：Excellent　B：Good　C：Fair　D：Poor

認めず，105%以上の悪化を認めた場合をPoor（図3-D）と評価した．

【結　果】

対象にした12症例は全例女性で，乳癌術後に発症していた．年齢は51～87才で，左上肢7例，右上肢5例であった．発症より手術までの期間は18ヶ月～29年であった（表1）．全症例においてPDEでリンパ管を確認することが可能であった．吻合出来たリンパ管の直径は約0.3～1.0mmで，吻合本数は1本が4例，2本が8例であり，部位別には手背~手関節部11本，前腕部5本，肘関節～上腕部4本であった．評価の結果はExcellent 5肢（42%），Good 4肢（33%），Fair 1肢（8%），Poor 2肢（17%）であった（表1）．ExcellentとGoodを有効としFairとPoorを無効と考えると，75%が有効で25%が無効であった．

【考　察】

従来，我々は四肢リンパ浮腫に対しKoshimaら[2]が報告したスーパーマイクロサージャリーテクニックを用いたリンパ管静脈吻合術（LVA：lymphaticovenous anastomosis）を行ってきた．

しかし，LVAにおけるリンパ管の同定は術者の経験に左右されるところが大きく，またLVA後のリンパ液が確実に静脈内に入っていることを確認することは困難であった．

2006年4月に照喜納ら[6]が，ICG蛍光リンパ管造影法を下肢リンパ浮腫症例のLVAに用いた報告をきっかけに，我々もLVAにPDEを用いたICG蛍光リンパ管造影法を導入した．

PDEを用いる事により，術中にリアルタイムに流れのあるリンパ管を確認出来るようになり，また吻合直後にリンパ管から静脈内にリンパ液が入っている

表1：症例一覧

症例	性別	年齢（歳）	患側	原疾患	放射線	化学療法	浮腫歴（ヶ月）	経過観察期間（ヶ月）	改善度（%）	評価
1	女性	87	左	乳癌	＋	－	348	16	111	Poor
2	女性	62	左	乳癌	－	－	36	13	86	Excellent
3	女性	55	左	乳癌	＋	＋	84	12	97	Fair
4	女性	80	右	乳癌	＋	－	24	5	93	Good
5	女性	55	左	乳癌	＋	－	240	13	86	Excellent
6	女性	75	右	乳癌	－	－	48	13	87	Excellent
7	女性	78	左	乳癌	＋	－	204	11	92	Good
8	女性	54	左	乳癌	－	＋	72	13	106	Poor
9	女性	68	右	乳癌	－	＋	32	10	95	Good
10	女性	60	右	乳癌	＋	－	18	9	89	Excellent
11	女性	63	右	乳癌	＋	－	178	10	88	Excellent
12	女性	51	左	乳癌	－	－	48	5	94	Good

ことを確認できるためLVAがより確実になってきた．特に皮切を加えた後もリンパ管をPDEで観察しながら追いかけられることは特記すべき点である．問題点としては深さ約2cmまでしか観察出来ないために，より深部のリンパ管を探す場合にはどうしても経験にもとづいて皮切を加えた後に，PDEで観察することになる点である．

ICG蛍光リンパ管造影法が導入される以

前の報告では，O'Brienら[4]は，上肢リンパ浮腫22例に対しLVAを行い，12例（55%）で平均38%の容量の低下をみたと報告している．Koshimaら[2]は，上肢リンパ浮腫12症例を対象に，経過観察期間1ヶ月～6年（平均2.2年）で，前腕（肘から10cm遠位）において，0～8cm（平均4.1cm）の減少が得られ，4cm以上の減少がみられたのは7例（58.3%）であったと報告している．これらの報告は評価法に違いがあり，今回の結果と直接比較することは困難であるが，我々の結果と同様にLVAの有効性を示したものと考えられる．

リンパ管静脈吻合の本数に関しては，我々は1肢に対し平均1.7本のリンパ管静脈吻合を行い，12例中9例でGood以上の結果を得た．リンパ管静脈吻合を数多く行ったほうがよいとの報告もある[1)5)]が，光嶋ら[3]はリンパ液の漏出が良好なリンパ管を見出せば1本のリンパ管静脈吻合でも術後に著明な改善が得られたと報告している．今回ICG蛍光リンパ管造影法を用いる事により，まだリンパ管としての機能を残しているリンパ管を見つけ出し皮静脈に吻合できた事により良好な結果が得られたものと考えられる．

【結　論】

1. 上肢リンパ浮腫症例12例に対しICG蛍光リンパ管造影法を用いたLVAを施行した．
2. 全例においてPDEでリンパ管を確認することができた．
3. LVAにおいて，ICG蛍光リンパ管造影法を用いることにより，リンパ管の同定が容易となり，静脈との吻合がより確実になった．

【文　献】

1) Huang GK : Microlymphaticovenous anastomosis for treating lymphedema. J Jpn Soc Plast Reconstr Surg, 7: 905-911, 1987.
2) Koshima I, Inagawa K, Urushihara K, et al.: Supermicrosurgical lymphaticovenular anastomosis for the treatment of lymphedema in the upper extremities. J Reconstractr Microsurg, 16: 437-442, 2000.
3) 光嶋　勲, 森口隆彦, 梶原康正: リンパ浮腫の治療. 手術, 50: 1715-1723, 1996.
4) O'Brien BM, Sykes PJ, Threlfall GN, et al.: Microlymphaticovenous anastomoses for obstructive lymphedema. Plast Recostr Surg, 60: 197-211, 1977.
5) 寺田　康, 井島　宏, 堀原　一: リンパ浮腫に対するリンパ管静脈吻合術. 外科, 50: 165-168, 1988.
6) 照喜納光信, 高見昌司, 諸岡久香, ほか: ICG蛍光リンパ管造影法を用いたリンパ管静脈吻合術. 第49回日本形成外科学会総会・学術集会抄録集: 191, 2006.

Scand J Plast Reconstr Surg Hand Surg, 2009; 43: 54–57

informa
healthcare

CASE REPORT

Reconstruction of adult auricular defect with thin titanium mesh and prelaminated free radial forearm flap

TATEKI KUBO, KOICHI TOMITA, AKIYOSHI TAKADA, KENJI YANO & KO HOSOKAWA

Department of Plastic Surgery, Osaka University Graduate School of Medicine, Osaka, Japan

Abstract
We used a thin titanium mesh combined with a prelaminated free radial forearm flap to construct a framework to reconstruct a traumatic defect in an adult ear. The prelaminated forearm flap covered both the anterior and posterior aspects of the titanium framework. A raised ear could therefore be created.

Key Words: *Adult auricular defect, pre-laminated free radial forearm flap, titanium mesh*

Introduction

Reconstruction of the ear remains one of the most challenging procedures encountered by reconstructive surgeons. A total auricular defect, usually traumatic or ablative in origin and usually encountered in adults, is reconstructed differently from congenital microtia. First, in such an acquired defect, there is usually less skin than in microtia, and so it is necessary to augment more. Secondly, because the rib cartilage in adults is often calcified, solid, and easily broken, it is difficult to bend and carve it to create a fine cartilaginous framework for the ear. In such acquired cases, therefore, instead of rib cartilage, alloplastic material and a porous polyethylene framework are used and combined with a temporoparietal fascial flap and skin graft to cover them [1,2].

However, there are two major potential problems with the use of porous polyethylene for the temporoparietal fascial flap. First, if the porous polyethylene framework is exposed, the whole framework may have to be removed. Secondly, in severe trauma or after ablation, the superficial temporal vessels are damaged and cannot be used for reconstruction. However, recent experience with orbital fractures and maxillary reconstruction have shown that exposure of titanium mesh plate is not as bad as exposure of other types of implants [3–5], and can often be treated by partial excision rather than removal of the whole mesh plate, or even by conservative treatment [3]. To reconstruct an adult traumatic ear defect, therefore, we used titanium mesh to form the ear's framework, which is thin and soft enough to be bent readily with the fingers, instead of other alloplastic material. To augment the skin, we used a prelaminated free radial forearm flap, in which the space for the titanium mesh implantation was prepared between the skin and pedicled radial vessels.

Case report

A 56-year-old Japanese man with right total auricular defect as a result of a road crash was referred to our department (Figure 1). He could not wear glasses, and also required cosmetic improvement.

Considering his age, we planned to use alloplastic material. We selected titanium mesh 0.1 mm thick (Titanium Micromesh, Unimedic, Osaka, Japan) as a framework for the ear because it is thin and soft

Presented at the 31st Annual Meeting of Japanese Society of Reconstructive Microsurgery in Kumamoto, Japan, October 15, 2004.

Correspondence: Tateki Kubo, MD, PhD, Department of Plastic Surgery, Osaka University Graduate School of Medicine, 2-2-C11 Yamadaoka, Suita-shi, Osaka 565-0871, Japan. Tel: +81 6 6879 6056. Fax: +81 6 6879 6059. E-mail: tateki@psurg.med.osaka-u.ac.jp

(Accepted 31 January 2007)

ISSN 0284-4311 print/ISSN 1651-2073 online
DOI: 10.1080/02844310701384025

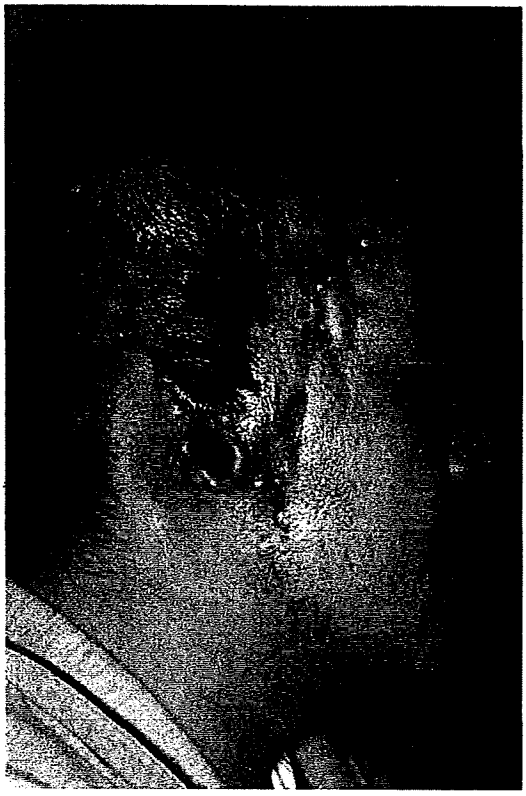

Figure 1. Preoperative view of the patient.

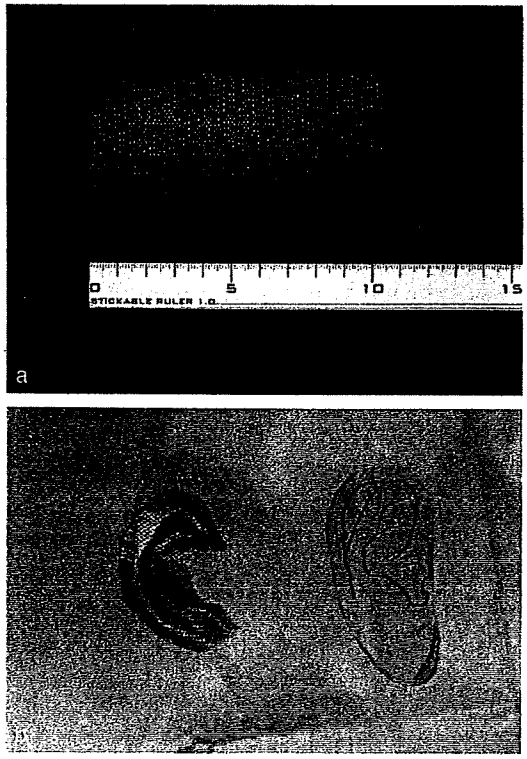

Figure 2. (*a*, *b*) A titanium mesh 0.1 mm thick and a framework for the ear.

enough to be bent easily with the fingers and forceps and to be cut with scissors (Figure 2). To cover this a temporoparietal fascial flap and a skin graft are commonly used. However, in this case, the superficial temporal vessels had been damaged, and so we selected a prelaminated free radial forearm flap, in which the space for the titanium mesh implant was prepared between the skin and pedicled radial vessels.

The first stage was done under local anaesthesia, the radial forearm skin undermined just below the skin, and a tissue expander (75 ml) inserted to make a space where a titanium framework could be implanted during the second stage (Figure 3*a*). After gradual infusion of 70 ml of saline solution during the next two months (Figure 3*b*), the radial forearm flap with the tissue expander was raised, and the radial artery and its vena comitantes were anastomosed end-to-end to the right facial artery and vein, respectively (Figure 3*c*). The tissue expander was then removed, and the titanium mesh framework inserted into the space. The expanded forearm flap covered both the anterior and posterior aspects of the titanium framework, and so a raised ear was created (Figure 4).

Three years after the second operation, there was no exposure of the titanium mesh framework in the reconstructed ear, and no inconvenience while wearing glasses. He was also satisfied cosmetically.

Discussion

Reconstruction of a total auricular defect in an adult is a complex challenge. Either rib cartilage or alloplastic materials are usually used for such a reconstruction, but although rib cartilage can provide an ideal framework for reconstruction of microtia in younger patients, its applications are limited in adult patients because the ribs have often become calcified [1]. Wellisz reported the successful reconstruction of 26 burned ears with alloplastic material (a porous polyethylene framework) combined with a temporoparietal fascial flap and skin graft [1].

In our case, we used thin titanium mesh to make the framework because it is chemically inert and not affected by soft tissues, it provokes little foreign-body or hypersensitivity reaction, and is easy to trim and mold [4]. Recent experiences with orbital fractures and maxillary reconstruction have shown that exposure of the titanium mesh plate is less problematic than that of other types of implant [3–5], and can often be treated by partial excision rather than removal of the whole mesh plate, or even conservatively [3].

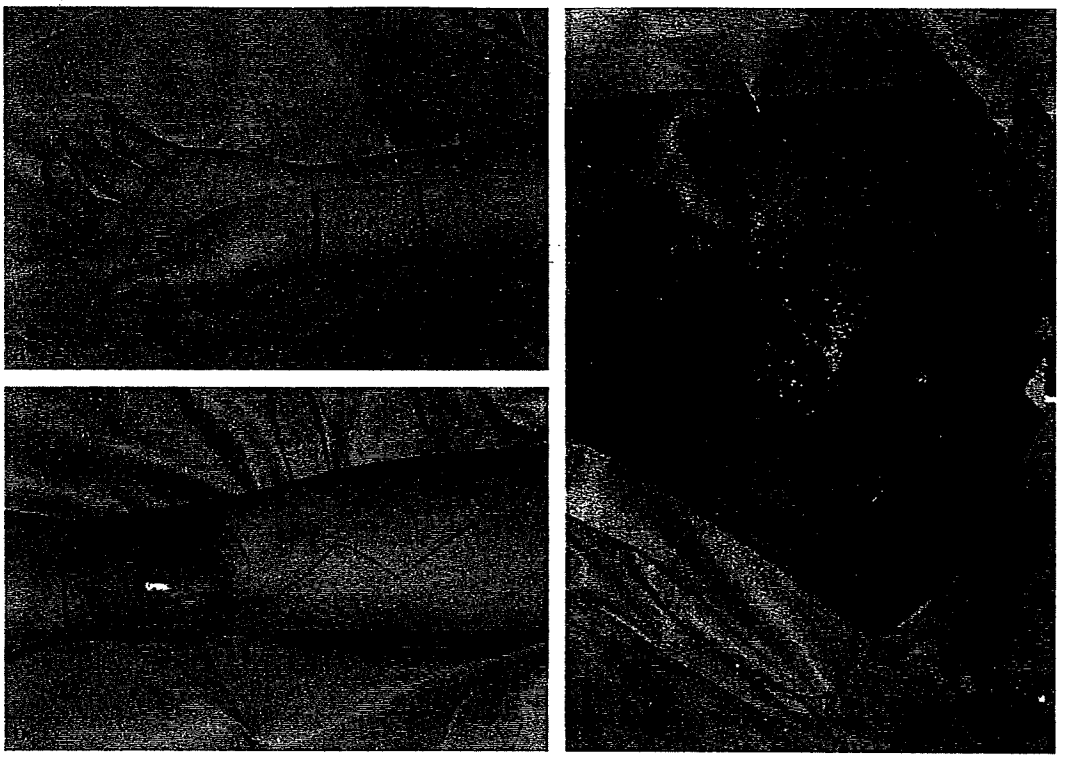

Figure 3. (*a*) The design for undermining the area to insert the tissue expander. Note that the radial artery lies right in the middle of the undermined area. (*b*) A tissue expander was infused over two months. (*c*) The radial forearm flap with the tissue expander was raised, and the radial artery and vena comitantes were anastomosed to the right facial artery and vein, respectively.

Figure 4. (*a, b*) Postoperative view of the patient eight months later.

Titanium mesh allows ingrowth of the vascular and soft tissue from the surrounding tissue through its pores, and prevents infection. Our patient has no sign of exposure three years later. The reconstructed ear is also flexible because of the nature of the thin titanium mesh.

The flaps that cover the implant must be neither too thin (for fear of the potential risk of exposure), nor too thick (to show the fine contour of the ear framework). Wellisz used a temporoparietal fascial flap and skin graft to cover his implants [1]. However, in cases where the superficial temporal vessels are not available, as ours, free flap transfer should be considered. Previous reports have shown the successful use of a free temporoparietal fascial flap from the other side [6], a free omental flap [7], a free forearm fascial flap [8], and a prelaminated free forearm skin flap [9,10].

Our procedure is similar to the technique reported by Chiang recently, in which the transferred forearm skin covers both the front and back of the framework at the same time [10]. However, there is a major difference between Chiang's technique and ours. Chiang placed the tissue expander away from the radial artery to preserve its skin perforators. This required more delay, and eventually three staged operations were necessary. We created a subcutaneous pocket for the tissue expander just above the radial artery. Even if the skin perforators were cut to make a subcutaneous pocket, the forearm skin can still be nourished through the capsule formed around the tissue expander. We think that formation of this blood supply through the capsule is the purpose of prelamination. Our operation requires two stages, but this is the same as required in the conventional microtia operation, which needs grafting of rib cartilage and raising of the ear.

To the best of our knowledge, this is the first description of a titanium mesh being used for reconstruction of an adult ear. Of course, there is a potential risk of exposure as long as a foreign body is used, but in selected cases (such as elderly patients), it is useful for total reconstruction of the adult ear.

References

[1] Wellisz T. Reconstruction of the burned external ear using a Medpor porous polyethylene pivoting helix framework. Plast Reconstr Surg 1993;91:811–8.

[2] Brent B. Microtia repair with rib cartilage grafts: a review of personal experience with 1000 cases. Clin Plast Surg 2002;29:257–71, vii.

[3] Nakayama B, Hasegawa Y, Hyodo I, et al. Reconstruction using a three-dimensional orbitozygomatic skeletal model of titanium mesh plate and soft-tissue free flap transfer following total maxillectomy. Plast Reconstr Surg 2004;114: 631–9.

[4] Hashikawa K, Tahara S, Ishida H, et al. Simple reconstruction with titanium mesh and radial forearm flap after globe-sparing total maxillectomy: a 5-year follow-up study. Plast Reconstr Surg 2006;117:963–7.

[5] Sugar AW, Kuriakose M, Walshaw ND. Titanium mesh in orbital wall reconstruction. Int J Oral Maxillofac Surg 1992; 21:140–4.

[6] Park C, Suk Roh T. Total ear reconstruction in the devascularized temporoparietal region: I. Use of the contralateral temporoparietal fascial free flap. Plast Reconstr Surg 2001;108:1145–53.

[7] Park C, Roh TS, Chi HS. Total ear reconstruction in the devascularized temporoparietal region: II. Use of the omental free flap. Plast Reconstr Surg 2003;111:1391–9.

[8] Bhandari PS. Total ear reconstruction in post burn deformity. Burns 1998;24:661–70.

[9] Akin S. Burned ear reconstruction using a prefabricated free radial forearm flap. J Reconstr Microsurg 2001;17:233–6.

[10] Chiang YC. Combined tissue expansion and prelamination of forearm flap in major ear reconstruction. Plast Reconstr Surg 2006;117:1292–5.

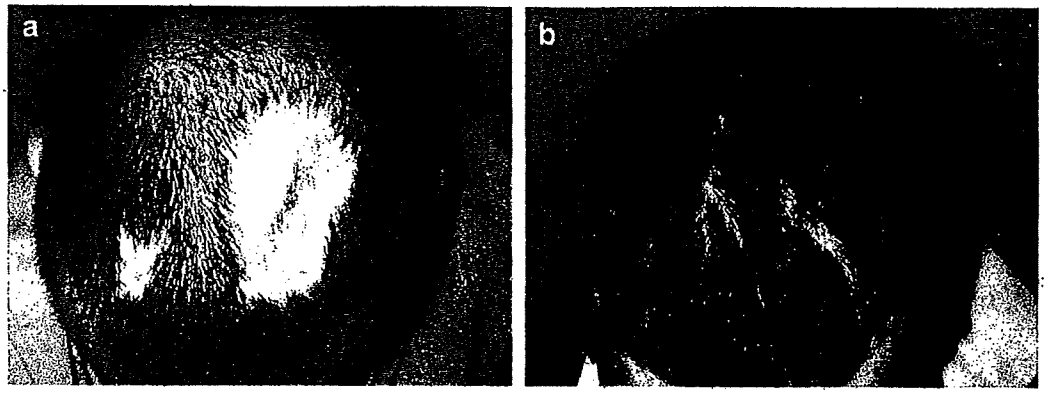

Figure 1 (a) Preoperative scalp alopecia. (b) Post-operative result, note the normal direction of the hair growth.

Figure 2 (a) Preoperative scalp alopecia. (b) Immediate post-operative result following advancement of tissue expanded skin with dog ear at the base of the flap in the right temple. (c) Post-operative result at 6 months where the dog ear has resolved with correct orientation of the direction of hair growth.

using the expanded scalp as either a rotation[2] or transposition flap.[3] Though these flaps maximise the use of the expanded tissue they cause misalignment of the direction of growth of the hair which leads to an unnatural looking result. Critics of advancing expanded scalp flaps argue that the dog ears resulting from this approach reduce the total surface area of expanded scalp available for use.[4] Even proponents of advancement flaps modify their techniques and try to minimise dog ears through the use of back cuts and interposition of local tissue to the base and sides of the flap.[5] We feel that this is unnecessary as dog ears following advancement of tissue expanded scalp skin will resolve with time and do not need surgical correction at either the primary procedure or at a later stage. In addition, advancement simplifies the preoperative planning for the procedure with regards to the placement of the tissue expander and the total amount of expanded skin needed for the reconstruction. To obtain optimal results for the treatment of alopecia with tissue expanded scalp flaps, our current practice is to advance our flaps with no surgical correction of dog ears. This is demonstrated in the two following cases (Figures 1 and 2).

References

1. Leedy JE, Janis JE, Rohrich RJ. Reconstruction of acquired scalp defects: an algorithmic approach. *Plast Reconstr Surg* 2005; 116:54e–72e.
2. Wells MD. Scalp reconstruction. In: Mathes SJ, editor. *Plastic surgery*. 2nd ed. Philidelphia: Saunders; 2007. p. 607–32.
3. Bauer BS, Margulis A. The expanded transposition flap: shifting paradigms based on experience gained from two decades of pediatric tissue expansion. *Plast Reconstr Surg* 2004;114:98–106.
4. Joss GS, Zoltie N, Chapman P. Tissue expansion technique and the transposition flap. *Br J Plast Surg* 1990;43:328–33.
5. Hudson DA. Maximising the use of tissue expanded flaps. *Br J Plast Surg* 2003;56:784–90.

N. White
S. Srivastava
Department of Plastic Surgery, University Hospitals Coventry and Warwickshire NHS Trust, Clifford Bridge Road, Coventry CV2 2DX, UK
E-mail address: nicholas.white@uhcw.nhs.uk

doi:10.1016/j.bjps.2007.12.063

Lint in the belly button

Sir:

The transverse rectus abdominis musculocutaneous (TRAM) flap or the deep inferior epigastric perforator (DIEP) flap

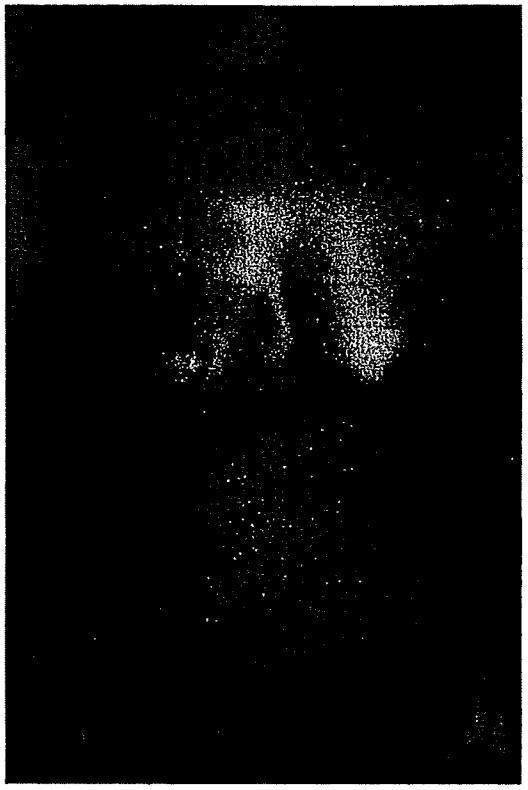

Figure 1 Donor site disruption and two-stage skin grafting made poor cosmetic result despite for esthetic purposes.

Table 1 The culture of organisms of lint in 24 cases

Patients	CNS	CB	SE	SA	GDE	Ac.L	Kl.O	Ps.A
1								O
2	O	O						
3	O	O				O		
4	O	O						
5		O		O				
6	O	O						
7	O	O						
8		O						
9	O							
10	O	O						
11	O	O						
12	O	O						
13	O	O						
14								O
15	O	O						O
16	O	O						
17	O	O						
18	O	O						
19				O				
20	O	O						
21	O	O					O	
22		O	O					
23	O				O			
24	O							

CNS, Coagulase-negative Staphylococcus; CB, Corynebacterium; SE, Staphylococcus Epidermidis; SA, Staphylococcus Aureus; GDE, group-D enterococcus; Ac.L, Acinetobacter Lwoffi; Kl.O, Klebsiella oxitosa; Ps.A, Pseudomonas aeruginosa.

are excellent option for patients desiring autogenous breast reconstruction. In elevating those flaps, circumcised umbilicus is floating in operative field, and lint occasionally comes out of the umibilical fossa despite preoperative preparation.

One of our breast reconstructive patients developed an overwhelming abdominal wound infection and septicemia due to Pseudomonas aeruginosa isolated from lint. The bacterium of the same organism was detected from the culture of heavy and pure lint extracted during the operation. Donor site disruption and two-stage skin grafting made poor cosmetic result despite for esthetic purposes (Figure 1).

With this case as a start, we test the lint of preoperative 24 female patients undergoing TRAM or DIEP flaps to see the culture of organisms of lint (Table 1).

Surprisingly some patients had heavy lint cultures positive for abnormal inhabitant organisms of the skin such as Enterococcus, Klebsiella oxytoca, Acinetobacter, Pseudomonas aeruginosa. And many umbilicus were not able to be taken a look of the bottom because of their spirally structure.

Preoperative clean-up procedure for umbilicus is ordinarily performed, but especially elevating flap around umbilicus, it should be performed meticulously and thoroughly to achieve a cosmetic result.

Mamoru Kikuchi
Kenji Yano
Department of Plastic Surgery,
Osaka University Graduate School of Medicine,
2-2 C11, Yamadaoka,
Suita-shi, Osaka,
565-0871 Japan
E-mail address: kikuchi@psurg.med.osaka-u.ac.jp

doi:10.1016/j.bjps.2008.06.086

Neuroscience Letters 461 (2009) 36–40

Contents lists available at ScienceDirect

Neuroscience Letters

journal homepage: www.elsevier.com/locate/neulet

Effects of the *in vivo* predegenerated nerve graft on early Schwann cell migration: Quantitative analysis using S100-GFP mice

Koichi Tomita*, Yuki Hata, Tateki Kubo, Toshihiro Fujiwara, Kenji Yano, Ko Hosokawa

Department of Plastic Surgery, Osaka University, Graduate School of Medicine, 2-2 C11 Yamadaoka, Suita-shi, Osaka 565-0871, Japan

ARTICLE INFO

Article history:
Received 25 February 2009
Received in revised form 26 April 2009
Accepted 26 May 2009

Keywords:
Schwann cell
Nerve predegeneration
Migration
S100-GFP mice
Macrophage
Misdirection

ABSTRACT

In peripheral nerve transection injury, continuity of axons as well as that of the basal lamina is disconnected. In such case, migrating Schwann cells (SCs) would be the only axonal guidance at an early stage of regeneration. However, it takes a few days for the dedifferentiated SCs to start migration, while axonal growth begins a few hours after injury. Consequently, the axons without guidance extensively branch out and wander off at the lesion, resulting in aberrant reinnervation. Therefore, enhancing SCs migration could be an attractive therapeutic strategy. In this study, we investigated the effects of the *in vivo* nerve predegeneration on SC migration and the time course of these changes. In our analysis, we established a novel animal model by nerve transplantation from S100-GFP mice (in which SCs constitutively express green fluorescent protein driven by the S100B promoter), by which SC migration could be exclusively visualized. Our results showed that SCs acquire the maximal migration ability with 14-day predegeneration, but subsequently it gradually decreased. There was a correlation between the time course of the changes in SC migration and the number of activated macrophages. These findings suggest that using predegenerated nerve grafts in repairing the transected nerves could facilitate SC migration into the recipient nerve stump. This technique could be beneficial for early establishment of axonal guidance and possible functional improvement after transection injury.

In the peripheral nervous system, injury-induced axonal disconnection brings about Wallerian degeneration, followed by regeneration. The denervated Schwann cells (SCs) in the proximal and distal stumps begin to dedifferentiate, proliferate, migrate, and then form processes called Bungner bands [26]. Most importantly, these processes act as guides for the regenerating axons [25]. In crush injury, most of the basal lamina scaffolds remain intact, and the axons and SCs can extend and migrate along them. On the other hand, in transection injury, the continuity of basal lamina scaffolds is completely destroyed, resulting in slow axonal growth. Thus, enhancing SC migration seems an attractive therapeutic strategy for reparing a transected nerve gap by a nerve graft.

Many studies have revealed that nerve predegeneration (i.e., preconditioning of the nerve graft *in vivo* before harvest) has some positive effects on axonal growth [3,7,14,18,24]. These effects were attributed to the changes in the denervated SCs, such as increased release of neurotrophic factors [5] and high proliferation rate [14]. However, few studies have demonstrated the effect of nerve predegeneration on SC migration, especially *in vivo*. Nevertheless, there is difficulty in creating an appropriate *in vivo* model, because in transection injury, bidirectional migration occurs between the proximal and distal stumps, which make the evaluation complicated. In this study, we investigated how the *in vivo* nerve predegeneration influences the SC migration *in vitro* and *in vivo*. A novel animal model was established by nerve transplantation from S100-GFP mice in which SCs constitutively express green fluorescent protein (GFP) driven by the S100B promoter. Furthermore, we assessed the correlation of SC migration ability with the extent of macrophage infiltration into the graft.

All animal experiments were approved by the Ethics Review Committee for Animal Experiment of Osaka University. Adult Sprague-Dawley rat sciatic nerves were transected at 0-, 7-, 14-, 28- and 56-day prior to assay. The sciatic nerves were separated and cleared of the blood vessels, muscles, and epineural sheaths. After fine cutting, the sciatic nerve explants were placed on poly-L-lysine-coated chamber slides in DME containing 10% FCS (Invitrogen), and incubated at 37 °C and 5% CO_2. Since no migrating cells were found after 24–48 h incubation except in 7- and 14-day predegenerated nerves, a 72 h assay was performed. Then, the explants were fixed in 4% paraformaldehyde, and immunostained with S100 antibody (Abcam, 1:100) followed by an Alexa fluor 488-labeled anti-mouse IgG (Molecular Probes). The maximum and mean distances between the migrating cells and the outer edge of explants were measured in each experiment.

S100-GFP mice [30] were obtained from the Jackson Laboratory (Bar Harbor, USA). We modified the GFP transgenic rat graft

* Corresponding author. Tel.: +81 6 6879 6056; fax: +81 6 6879 6059.
E-mail address: tomita@psurg.med.osaka-u.ac.jp (K. Tomita).

0304-3940/$ – see front matter © 2009 Elsevier Ireland Ltd. All rights reserved.
doi:10.1016/j.neulet.2009.05.075

model previously described [16]. Briefly, heterozygous S100-GFP mice (20–25 g) were deeply anesthetized by intraperitoneal injection of sodium pentobarbital (40 mg/kg). The sciatic nerve was exposed in the upper thigh and then transected at the sciatic notch. The proximal nerve stump was turned 180° and sutured to the muscle to prevent reinnervation. After 0-, 7-, 14-, 28-, and 56-day of degeneration, the common peroneal (CP) nerve was exposed and a 3-mm-long segment of the CP nerve was harvested. Then, the CP nerve of the GFP(−) littermates (20–25 g) was exposed and transected approximately 1 mm from its branching point from the sciatic nerve, and the predegenerated nerve graft was placed in the gap. Fibrin glue was prepared immediately before use by combining equal parts of thrombin, fibrinogen and fibronectin (Sigma–Aldrich, USA). A volume of 10 μL was applied to the surgical repair site, securing both ends of the graft. Four days after surgery, the mice were anesthetized and perfused with phosphate buffer saline (PBS) followed by 4% paraformaldehyde The entire CP nerve was harvested from the animal, and whole mount fluorescent preparations were made. The profiles of GFP(+) SCs migrating proximally and distally to the graft could be followed using a laser confocal microscope (Zeiss, LSM 510). The maximum migration distance from the proximal stump of the graft was assessed in each animal.

Immunohistochemistry was also performed on the predegenerated nerve grafts and the transplanted nerves. The specimens were harvested from predegenerated S100-GFP mice (CP nerve) or transplanted mice (CP nerve including the graft) and fixed overnight. For immunostaining, tissues were prepared as 12 μm cryostat sections after cryoprotection (30% sucrose) and embedding in OCT compound (TissueTek). Immunostaining was performed as previously described [28]. The following primary antibodies were utilized at the indicated dilutions: mouse anti-S100 (1:100; Abcam); rat monoclonal to macrophage (F4/80; 1:1000, Abcam); rabbit anti-neurofilament H (1:500, Chemicon). To count the number of macrophages in the predegenerated CP nerves of the S100-GFP mice, the nerves were harvested at a point 5 mm distal from the site of transection. The macrophages in the endoneurium were recognized using anti-F4/80 antibody, and in each predegeneration period, the positively stained cells were manually counted in the randomly selected three microscopic fields (100 μm × 100 μm) from four sections. All data were expressed as the mean ± SEM. Statistical analysis was performed using one-way ANOVA followed by *post hoc* Tukey test to determine the statistical significance between the data sets, ($^{*}P < 0.05$ was considered as significant).

We first examined the effect of the *in vivo* predegeneration on SC migration *in vitro* by explants migration assay. In 0-day predegenerated nerve (i.e., fresh nerve), no migrating cells were found within 72 h of incubation (Fig. 1A), whereas dramatically increased migration of S100(+) SCs was observed in 7-day (max: 562 ± 64 μm; mean: 208 ± 6 μm, five explants from 5 animals were used in each period) and 14-day (max: 594 ± 33 μm; mean: 285 ± 28 μm) predegenerated nerves (Fig. 1B and C). The migration distance peaked in the 14-day nerve, and then decreased in the 28-day nerve (max: 251 ± 34 μm; mean: 136 ± 11 μm), and finally reached zero in the 56-day nerve (Fig. 1B and C).

Next, we evaluated the influence of the *in vivo* predegeneration on SC migration *in vivo* (Fig. 2A). Since it takes at least a few days until the denervated SCs start to migrate in fresh nerve [8], we chose a 4-day *in vivo* interval to study the time course of the changes in early SC migration ability of the *in vivo* predegenerated nerve grafts. The longitudinal sections of the graft harvested on postoperative day 4 showed migration of the donor-derived GFP(+) cells from the cut ends into the recipient nerve along its long axis both proximally and distally (Fig. 2B). Immunostaining with anti-S100 antibody revealed colocalization of SCs marker S100 and GFP expressions, indicating that these migrating cells are SCs (Fig. 2C). While it has been reported that some macrophages in the S100-GFP line also express GFP [30], immunostaining with anti-F4/80 antibody, a marker for macrophages, showed few GFP(+) cells colocalized with F4/80 within recipient nerves (data not shown). These observations confirmed that our model is appropriate for the *in vivo* SC migration assay.

Because we considered that SC migration from the edge of graft into the proximal stump is important for early axonal growth, proximal migration was quantitatively assessed by preparing whole mount nerves, in which all the GFP(+) migrating cells could be observed using confocal microscopy (Fig. 2D). Consistent with the *in vitro* assay, 0-day predegeneration revealed few migrating SCs on postoperative day 4, and the maximum migration distance was 147 ± 10 μm (five animals were used in each period, Fig. 2E). In contrast, SCs with 7-day predegeneration showed dramatically long migration distance (748 ± 47 μm), and reaching a peak on 14-day (959 ± 54 μm)(Fig. 2E). Consistent with the *in vitro*

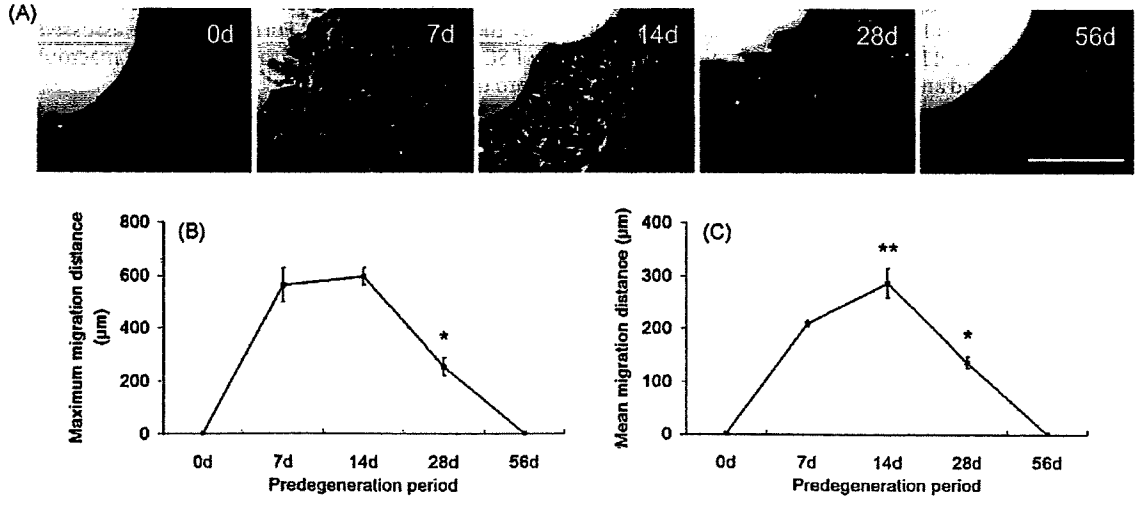

Fig. 1. The time course of the changes in the *in vivo* predegenerated SC migration ability *in vitro*. (A) Nerve explants assay was performed using 0-, 7-, 14-, 28-, and 56-day predegenerated rat sciatic nerve. (B, C) The maximum and mean migration distances from the edge of explants were measured. The 7- and 14-day predegeneration periods showed extensive SC migration, whereas no migrating cells were found in the 0- and 56-day predegeneration period. The data are mean ± SEM, five explants from 5 animals were used in each period. $^{*}P < 0.05$ as compared with the 7- and 14-day groups, $^{**}P < 0.05$ as compared with the 7-day group (one-way ANOVA followed by *post hoc* Tukey test).

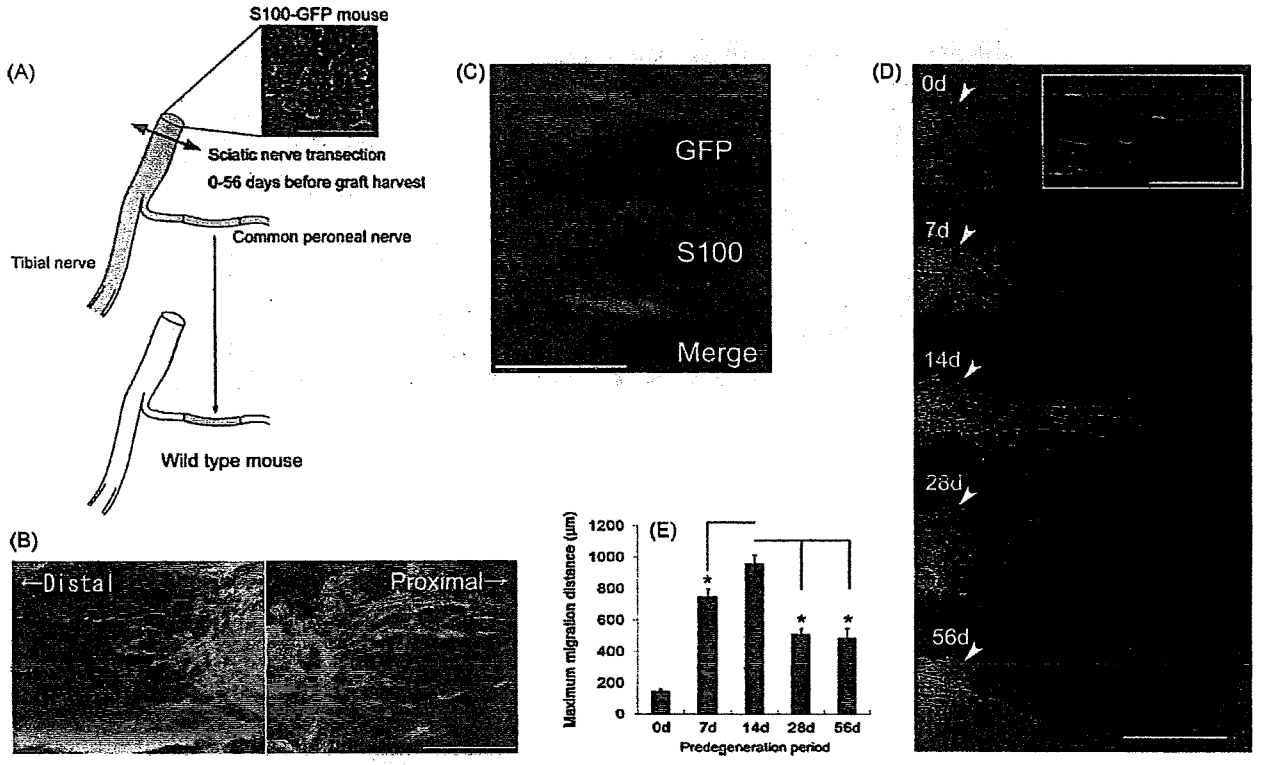

Fig. 2. *In vivo* SC migration assay using the S100-GFP mice graft model. (A) A schematic illustration of the protocol of experimental animal model is shown. After conditioning the CP nerve of the S100-GFP mice for 0-, 7-, 14-, 28-, and 56-day, a 3-mm segment of the nerve was interposed between the gap created in the CP nerve of GFP(−) wild type mice. Small panel shows the cross section of sciatic nerve immunostained with anti-neurofilament antibody (red). Bar; 50 μm. (B) Cryostat sections showed that GFP(+) cells migrated from the edge of graft into the recipient nerve stumps both proximally and distally, forming the Bungner bands. Bar; 150 μm. (C) Colocalization of S100 immunostaining with GFP(+) cells was found in the recipient nerves, confirming that these migrating cells are SCs. Bar; 50 μm. (D) The grafts were harvested on postoperative day 4, and whole mount specimens were prepared. Whole images of proximally migrating SCs were obtained from adjacent microscopic fields and combined together. The arrow heads point to the proximal coaptation sites in the graft. Small panel shows the high magnification view of SCs migrating from 14-day graft. Bar; 500 μm (large panel), 100 μm (small panel). (E) The maximum SC migration distance from the proximal graft ends was assessed. The 14-day predegeneration showed significantly longer distance as compared with the other groups. The data are mean ± SEM, five animals were used in each period. $^*P < 0.05$. (one-way ANOVA followed by post hoc Tukey test). (For interpretation of the references to color in this figure legend, the reader is referred to the web version of the article.)

assay, the SC migration distance significantly decreased on 28-day (508 ± 36 μm) and on 56-day (486 ± 62 μm) (Fig. 2E).

Macrophage recruitment into the endoneurium of the lesioned nerve and its activation greatly influences the changes in SCs [19]. Thus, we finally assessed the time course of the changes in the number of macrophages in the predegenerated CP nerve of S100-GFP mice. In the 0-day predegenerated nerve, only a few slender ramified F4/80 stained macrophages were found within the endoneurium (Fig. 3A). In contrast, in the 7-day predegenerated nerve, the endoneurium was filled with foamy macrophages (Fig. 3A), and the density of macrophages peaked at 14-day (1350 ± 104 cells/mm^2, four animals were used in each period) (Fig. 3B), which is consistent with previous reports [2,27]. After the density slightly dropped on 28-day (1275 ± 85 cells/mm^2), it significantly decreased on 56-day (700 ± 71 cells/mm^2).

These results showed that SCs in the *in vivo* predegenerated nerve grafts acquire significantly high migration ability. This was evident with 7-day predegeneration, and the most significant effects could be obtained with 14-day predegeneration. In the animal model, with 7- or 14-day predegeneration, SCs could migrate and extend their processes into the proximal nerve stump over 700 μm within 4-day after injury, whereas few migrating SCs could be found with 0-day predegeneration. When peripheral nerves are transected, the axons grow along the Bungner bands formed by SCs and its basal lamina [15]. However, it takes at least a few days until SCs dedifferentiate and start to migrate, resulting in "the initial delay period" [8]. On the other hand, the peripheral neurites begin to regenerate and seek for distal pathways within a few hours after injury [24], although there would be no axonal guidance yet. Consequently, extensive axonal branching and lateral movement of the regenerating axons at the injured site, which are considered as causes of abnormal regeneration such as axonal misdirection, would occur [4,28,29]. Indeed, previous studies reported that rat sciatic nerve transection injury resulted in significantly increased number of myelinated axons in the distal nerve and impaired functional recovery as compared with crush injury, while the number of motoneurons from which axons had regenerated was not significantly different between the two groups [9,17]. Furthermore, other study revealed that misdirected axons were associated with misdirected SC processes, and the proportion of these axons was reduced by facilitating SC migration [6]. Therefore, early establishment of axonal guidance by grafting predegenerated nerve grafts could be beneficial not only for rapid axonal growth, but also for improving the quality of reinnervation.

On the other hand, previous studies reported that a preconditioning lesion (i.e., a damage to the distal nerve precedes the testing lesion) of the optic nerve in goldfish resulted in a reduced initial delay and an accelerated axonal outgrowth [20,22]. In these studies, however, the testing lesion was performed by crush injury in which the basal lamina scaffolds remain intact. Therefore, it is unclear if these effects would also occur in transection injury in which no axonal guidance is present within a few days after injury.

Another interesting finding in this study was that the changes in the SC migration ability in the predegenerated nerve grafts correlated with the time course of the changes in the number of endoneurial macrophages, suggesting a possible relationship

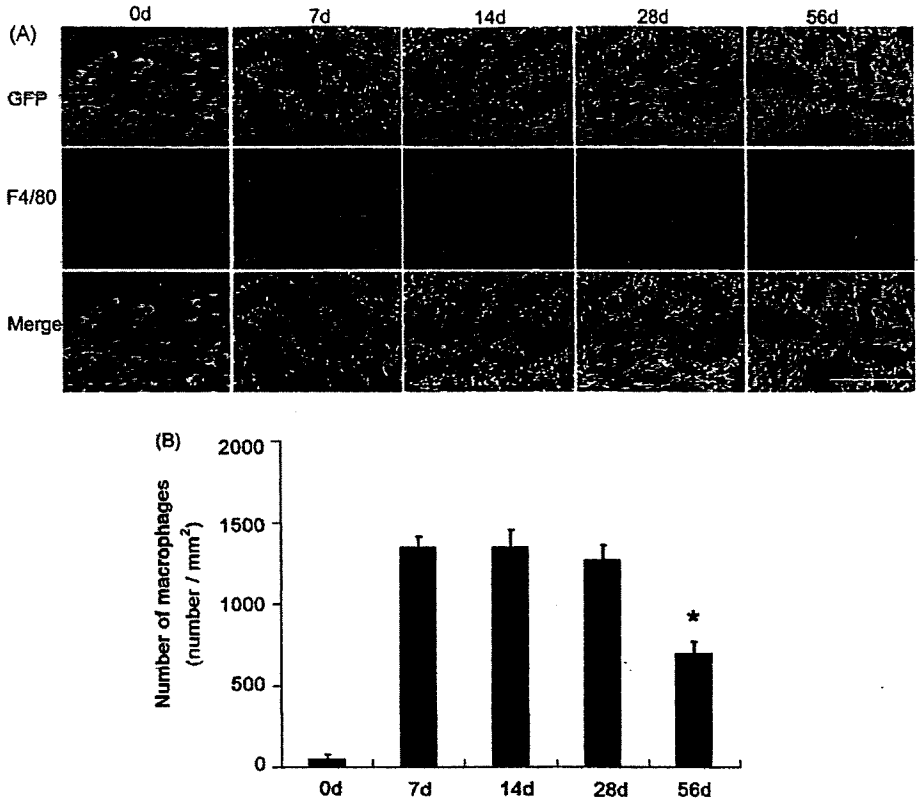

Fig. 3. The time course of the changes in the number of endoneurial macrophages was assessed in the *in vivo* predegenerated CP nerves of S100-GFP mice. (A) Few F4/80(+) macrophages were found in the fresh nerve, whereas many foamy, sponge-like macrophages were found in the 7-day predegenerated nerve. Later on, these cells decreased on 56-day. Bar; 150 μm. (B) The density of the infiltrating macrophages was assessed. The 56-day predegenerated nerve showed a significantly small value as compared with the 7-, 14- and 28-day predegenerated nerves. The data are mean ± SEM, four animals were used in each period. $^{*}P < 0.05$ as compared with 7-, 14-, and 28-day (one-way ANOVA followed by *post hoc* Tukey test).

between the SC migration ability and the activated macrophages recruited from the circulation. During Wallerian degeneration and subsequent regeneration, interactions between SCs and macrophages play an essential role [19,23]. For instance, the expressions of MCP-1, MIP-1α, TNF-α, IL-1α,and IL-1β in SCs reportedly induce macrophage recruitment into the injured nerve within 3-day after injury [13,19,21,23], resulting in myelin phagocytosis by the activated macrophages. Regarding the effects of the activated macrophages on the SC migration, NGF, whose synthesis is up-regulated in SCs after transection injury, promotes SC migration [1], and its synthesis is reportedly regulated by infiltrating macrophages [11]. Other investigators suggested that the oxidized galectin-1, of which the reduced form was originally released by SCs and injured axons, stimulates the macrophages to secrete a factor which promotes SC migration [10,12], while the corresponding factor has not been determined yet. Therefore, local application of activated macrophages to the lesion may be a possible therapeutic strategy for treating a peripheral nerve transection injury.

In summary, we have shown that the *in vivo* nerve predegeneration significantly enhances SC migration both *in vitro* and *in vivo*. Our *in vivo* model demonstrated that SCs in the predegenerated nerve graft migrated into the proximal nerve stump as early as 4-day after injury, which might accelerate the early axonal growth and reduce the initial delay period. This effect was evident with 7-day predegeneration and the maximal effect was observed at 14-day. Further studies are necessary to elucidate how these effects influence the functional recovery after peripheral nerve transection injury, especially on the quality of reinnervation such as reduction of axonal misdirection.

Acknowledgments

This work was funded by the Research Grant from the Japanese Ministry of Education, Science, Sports and Culture (18791319) and the General Insurance Association of Japan to K. T. The authors sincerely thank Professor Masaya Tohyama (Department of Anatomy and Neuroscience) for his support during this study.

References

[1] E.S. Anton, G. Weskamp, L.F. Reichardt, W.D. Matthew, Nerve growth factor and its low-affinity receptor promote Schwann cell migration, Proc. Natl. Acad. Sci. U.S.A. 91 (1994) 2795–2799.
[2] A.M. Avellino, D. Hart, A.T. Dailey, M. MacKinnon, D. Ellegala, M. Kliot, Differential macrophage responses in the peripheral and central nervous system during wallerian degeneration of axons, Exp. Neurol. 136 (1995) 183–198.
[3] J.A. Bertelli, M. Taleb, J.C. Mira, M.F. Ghizoni, Functional recovery improvement is related to aberrant reinnervation trimming. A comparative study using fresh or predegenerated nerve grafts, Acta Neuropathol. 111 (2006) 601–609.
[4] T.M. Brushart, Motor axons preferentially reinnervate motor pathways, J. Neurosci. 13 (1993) 2730–2738.
[5] S. Carbonetto, Facilitatory and inhibitory effects of glial cells and extracellular matrix in axonal regeneration, Curr. Opin. Neurobiol. 1 (1991) 407–413.
[6] Y.Y. Chen, D. McDonald, C. Cheng, B. Magnowski, J. Durand, D.W. Zochodne, Axon and Schwann cell partnership during nerve regrowth, J. Neuropathol. Exp. Neurol. 64 (2005) 613–622.
[7] L.B. Dahlin, Prevention of macrophage invasion impairs regeneration in nerve grafts, Brain Res. 679 (1995) 274–280.
[8] N. Danielsen, J.M. Kerns, B. Holmquist, Q. Zhao, G. Lundborg, M. Kanje, Predegeneration enhances regeneration into acellular nerve grafts, Brain Res. 681 (1995) 105–108.
[9] G.C. de Ruiter, M.J. Malessy, A.O. Alaid, R.J. Spinner, J.K. Engelstad, E.J. Sorenson, K.R. Kaufman, P.J. Dyck, A.J. Windebank, Misdirection of regenerating motor axons after nerve injury and repair in the rat sciatic nerve model, Exp. Neurol. 211 (2008) 339–350.

[10] K. Fukaya, M. Hasegawa, T. Mashitani, T. Kadoya, H. Horie, Y. Hayashi, H. Fujisawa, O. Tachibana, S. Kida, J. Yamashita, Oxidized galectin-1 stimulates the migration of Schwann cells from both proximal and distal stumps of transected nerves and promotes axonal regeneration after peripheral nerve injury, J. Neuropathol. Exp. Neurol. 62 (2003) 162–172.
[11] R. Heumann, D. Lindholm, C. Bandtlow, M. Meyer, M.J. Radeke, T.P. Misko, E. Shooter, H. Thoenen, Differential regulation of mRNA encoding nerve growth factor and its receptor in rat sciatic nerve during development, degeneration, and regeneration: role of macrophages, Proc. Natl. Acad. Sci. U.S.A. 84 (1987) 8735–8739.
[12] H. Horie, T. Kadoya, N. Hikawa, K. Sango, H. Inoue, K. Takeshita, R. Asawa, T. Hiroi, M. Sato, T. Yoshioka, Y. Ishikawa, Oxidized galectin-1 stimulates macrophages to promote axonal regeneration in peripheral nerves after axotomy, J. Neurosci. 24 (2004) 1873–1880.
[13] S. Karanth, G. Yang, J. Yeh, P.M. Richardson, Nature of signals that initiate the immune response during Wallerian degeneration of peripheral nerves, Exp. Neurol. 202 (2006) 161–166.
[14] G. Keilhoff, H. Fansa, W. Schneider, G. Wolf, *In vivo* predegeneration of peripheral nerves: an effective technique to obtain activated Schwann cells for nerve conduits, J. Neurosci. Methods 89 (1999) 17–24.
[15] J.M. Kerns, N. Danielsen, B. Holmquist, M. Kanje, G. Lundborg, The influence of predegeneration on regeneration through peripheral nerve grafts in the rat, Exp. Neurol. 122 (1993) 28–36.
[16] A. Kimura, T. Ajiki, K. Takeuchi, Y. Hakamata, T. Murakami, Y. Hoshino, E. Kobayashi, Transmigration of donor cells involved in the sciatic nerve graft, Transplant. Proc. 37 (2005) 205–207.
[17] N. Lago, X. Navarro, Correlation between target reinnervation and distribution of motor axons in the injured rat sciatic nerve, J. Neurotrauma 23 (2006) 227–240.
[18] W. Marcol, K. Kotulska, M. Larysz-Brysz, I. Matuszek, E. Olakowska, J. Lewin-Kowalik, Extracts obtained from predegenerated nerves improve functional recovery after sciatic nerve transection, Microsurgery 25 (2005) 486–494.
[19] R. Martini, S. Fischer, R. Lopez-Vales, S. David, Interactions between Schwann cells and macrophages in injury and inherited demyelinating disease, Glia 56 (2008) 1566–1577.
[20] I.G. McQuarrie, B. Grafstein, Effect of a conditioning lesion on optic nerve regeneration in goldfish, Brain Res. 218 (1981) 253–264.
[21] F.E. Perrin, S. Lacroix, M. Aviles-Trigueros, S. David, Involvement of monocyte chemoattractant protein-1, macrophage inflammatory protein-1alpha and interleukin-1beta in Wallerian degeneration, Brain 128 (2005) 854–866.
[22] J.B. Reich, D.W. Burmeister, J.T. Schmidt, B. Grafstein, Effect of conditioning lesions on regeneration of goldfish optic axons: time course of the cell body reaction to axotomy, Brain Res. 515 (1990) 256–260.
[23] S. Shamash, F. Reichert, S. Rotshenker, The cytokine network of Wallerian degeneration: tumor necrosis factor-alpha, interleukin-1alpha, and interleukin-1beta, J. Neurosci. 22 (2002) 3052–3060.
[24] J. Sjoberg, M. Kanje, The initial period of peripheral nerve regeneration and the importance of the local environment for the conditioning lesion effect, Brain Res. 529 (1990) 79–84.
[25] Y.J. Son, W.J. Thompson, Schwann cell processes guide regeneration of peripheral axons, Neuron 14 (1995) 125–132.
[26] G. Stoll, H.W. Muller, Nerve injury, axonal degeneration and neural regeneration: basic insights, Brain Pathol. 9 (1999) 313–325.
[27] H.S. Taskinen, M. Roytta, The dynamics of macrophage recruitment after nerve transection, Acta Neuropathol. 93 (1997) 252–259.
[28] K. Tomita, T. Kubo, K. Matsuda, K. Yano, M. Tohyama, K. Hosokawa, Myelin-associated glycoprotein reduces axonal branching and enhances functional recovery after sciatic nerve transection in rats, Glia 55 (2007) 1498–1507.
[29] C. Witzel, C. Rohde, T.M. Brushart, Pathway sampling by regenerating peripheral axons, J. Comp. Neurol. 485 (2005) 183–190.
[30] Y. Zuo, J.L. Lubischer, H. Kang, L. Tian, M. Mikesh, A. Marks, V.L. Scofield, S. Maika, C. Newman, P. Krieg, W.J. Thompson, Fluorescent proteins expressed in mouse transgenic lines mark subsets of glia, neurons, macrophages, and dendritic cells for vital examination, J. Neurosci. 24 (2004) 10999–11009.

形成外科 52(6)：623～630，2009

特集 乳癌切除後の乳房再建—乳房インプラント vs 皮弁再建

有茎広背筋皮弁による再建

矢野健二*

Key words：乳房再建　広背筋皮弁　乳癌術後

はじめに

広背筋皮弁は乳房再建において最も利用されている自家組織の一つである[1)~10)]。その利点として以下の点が挙げられる。①位置的に腋窩部を支点として前胸部に移動できるため乳房部の再建に適している。②広背筋は広く薄い筋肉であるためその直上のどの部位に皮島を作製しても皮弁への血行は良好である。③広背筋採取による筋の機能的な脱落症状が少ない。④広背筋の採取創は背部で下着に隠れる部位であり患者にとっても目立たない。以上のような多くの利点を有しておりさまざまな形の乳房欠損に対する乳房再建に利用可能である。

本稿では広背筋皮弁を用いた著者の乳房再建手術方法と広背筋皮弁の適応，利点·欠点，合併症について述べる。

I 広背筋の解剖

広背筋は第6～8胸椎以下の棘突起，腰背腱膜浅葉，腸骨稜，第3～4の下位肋骨および肩甲骨下角から起こり，上部はほとんど水平に外方へ，下部は次第に斜め外上方へ向かう。停止部は，上腕骨の小結節稜である。主たる栄養血管は，腋窩動静脈の枝である肩甲下動静脈が肩甲回旋動静脈を分枝した後の胸背動静脈である。胸背動静脈だけで広背筋全体が栄養され，多数の筋肉皮膚穿通枝を分枝しており，広背筋上の広範な皮膚皮下組織も栄養されている。広背筋の運動支配神経は胸背神経である。

広背筋上皮膚の知覚を支配する神経はTh6～12の胸神経後枝である。胸神経後枝は胸椎の横突起間を通って体幹の後壁に出て，外側皮枝と内側皮枝とに分かれて，広背筋を貫き，直上の皮膚に分布する[11)12)]。

II 方　法

1. 皮弁のデザイン

広背筋皮弁採取における皮膚切開線は基本的にブラジャーラインに沿った横方向の紡錘形切開とするが，できるだけ多くの組織量を必要とする時は背部皮膚のしわの方向である斜め方向の皮膚切開とする[1)]。

2. 皮弁の切開

皮膚切開はほぼ垂直に浅筋膜まで行う。創縁の皮下脂肪組織を取りすぎると縫合時に真皮が下床の筋肉と癒着して陥凹瘢痕となり，術後に上肢の可動制限や背部皮膚の拘縮感を訴えることがある。

*大阪大学医学部形成外科

3. 広背筋皮弁の挙上

浅筋膜まで切開を加えて，浅筋膜下で剝離を行う。浅筋膜上の脂肪組織を付着すると背部の陥凹が目立つことがある。最初に頭側に向かって剝離を行い，上外側は乳癌切除時の創まで皮下トンネルを作製する。上内側は広背筋の上縁と僧帽筋の外側縁を確認する。

次に尾側に向かって同じ層で剝離して行くが，剝離する範囲は乳腺切除量に応じて決定する。乳腺切除量が少ない場合は皮島尾側端から 1～2 cm 剝離するだけでよいが，乳腺切除量が多い場合は広背筋全体を浅筋膜下で剝離する。そして広背筋の外側縁から胸壁側面（以下裏面）の剝離を行い，必要な位置で筋体の尾側を切離する。

次に筋体を尾側端から剝離して行く。この時に筋体裏面に脂肪組織を付着させ，剝離しやすい層で上方に剝離して行くと，前鋸筋や大菱形筋下の層に入っていくので注意が必要である。乳房外側の切開創のレベルまで筋体裏面を剝離したら，筋皮弁を乳房外側の創部から前方に引き出す。そこで術者は患者の前胸部に位置を変え，乳房欠損部外側の創から筋皮弁を欠損方向に引っ張りながら，剝離操作を続ける。

筋体裏面の剝離を腋窩方向に進めて行くと栄養血管である胸背動静脈が透けて見えてくる。それをさらに剝離していき，胸背動静脈が前鋸筋枝と分岐する部位を同定する。分岐部より少し末梢で胸背動静脈が筋肉内に埋入するため，分岐部より中枢側の胸背動静脈と筋体の隙間を剝離剪刀やモスキートペアンを用いて剝離し，筋体と神経血管束を完全に分離する。筋体と胸背動静脈の隙間に術者の左示指を挿入し，左示指よりも中枢側で広背筋の筋体を電気メスで離断する。筋体を乳房方向に伸展させ，まだ十分な可動性が得られない場合は，神経血管束周囲の結合組織を剝離剪刀で剝離し，緊張のある結合組織を切離する。この時点で，広背筋皮弁は神経血管束のみでつながった島状筋皮弁となり，筋皮弁を組織欠損部に充填する[1]。

4. 広背筋皮弁の充填法

広背筋皮弁の充填法は乳癌術式により多少異なる。基本的には切除される乳腺の大きさにより筋皮弁量を調整するが，乳腺の切除部位や乳房皮膚切除の有無により若干再建手技が異なる。

AC，CD 領域の乳房温存手術および skin-sparing mastectomy（以下 SSM）の再建は最も容易であり，挙上した広背筋皮弁を乳房外側の切開創から目的とする組織欠損部に充填するだけでよい。ポケット奥での縫合糸による組織の固定は特に行わず，筋肉の収縮による後戻り防止のためにポケット入口部での筋体の固定のみ行う。

AB 領域の乳房温存手術は CD 領域の乳腺脂肪組織が残存しているので，広背筋の筋体の一部がいったん CD 領域の残存乳腺下を通る。したがって，その部分の広背筋上には脂肪を付けないように薄くして，筋体を広げて通過させる。

BD 領域は広背筋皮弁を移動する際に最も遠い部位となるため，背部に作製する皮島の位置を通常よりやや尾側にデザインし，遠位部に最もボリュームが届くようにする。そして，通常より少し大きめに皮島をデザインする。C 領域の乳腺下または外側を通る広背筋はできるだけ薄い方がよいため，その部分は広背筋上に脂肪を付けないようにする。そして，この領域の再建における最も大事なポイントは皮弁の固定である。皮弁の固定が不十分な場合は術後の筋体の収縮により容易に乳房尾側半分の形態に変形を来たす。皮弁の固定は周囲の組織に縫合糸で固定するだけでは不十分であり，皮島を露出させて皮膚そのものを固定する必要がある。乳房の皮膚欠損がある場合はその部位に皮島を露出させて縫合

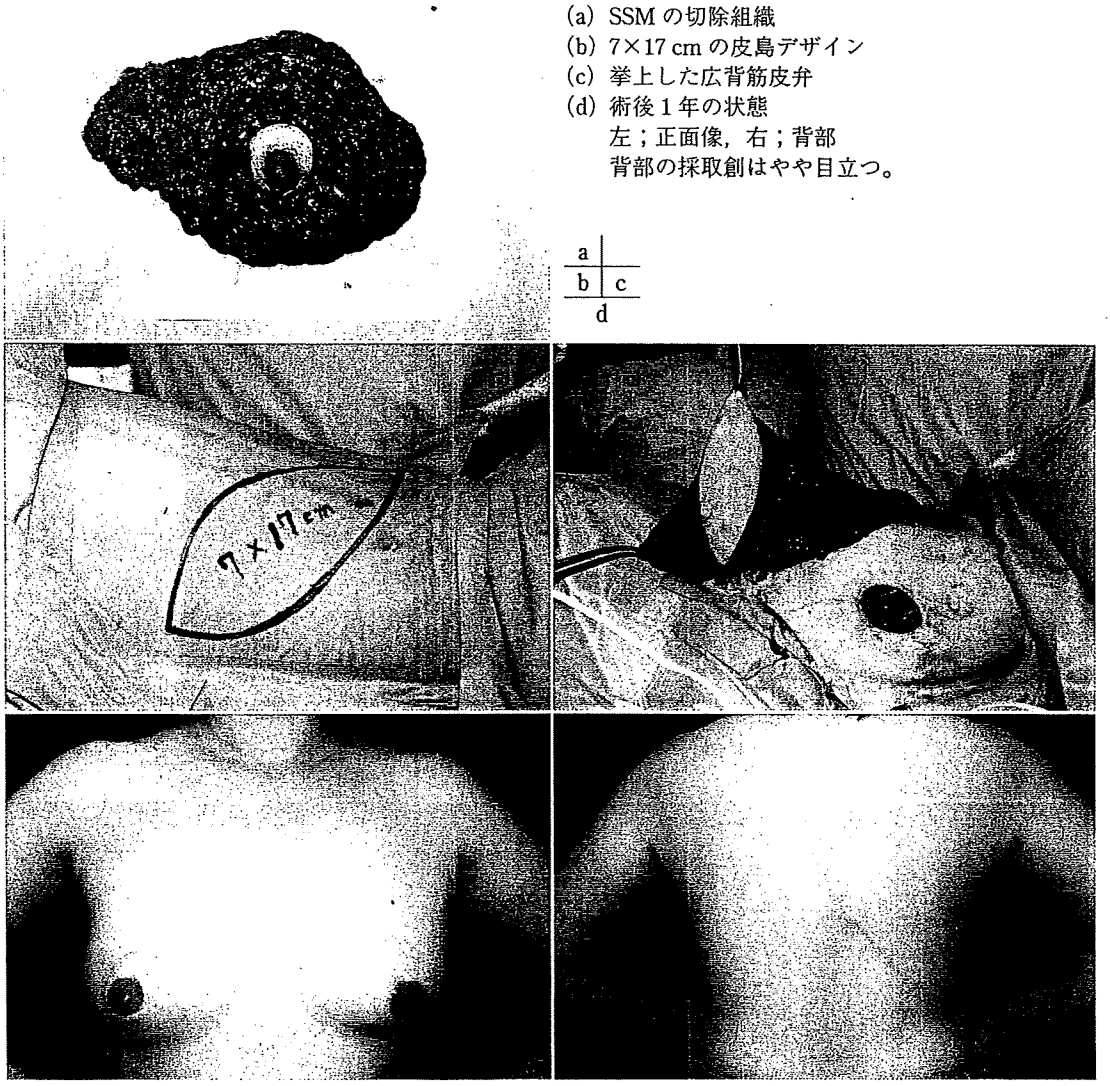

図1　症例1：右乳癌SSM後の一次再建症例（40歳）
(a) SSMの切除組織
(b) 7×17 cmの皮島デザイン
(c) 挙上した広背筋皮弁
(d) 術後1年の状態
左；正面像，右；背部
背部の採取創はやや目立つ。

固定すればよいが，皮膚欠損がない場合でも乳房下溝に小切開を加え，小さい皮弁を露出させて皮弁を縫合固定すると術後の筋体収縮による変形予防に効果的である[1]。

胸筋温存乳房切除術の再建は，乳房皮膚切除を行った部位に背部皮膚が露出する。乳癌切除前に乳房皮膚切開予定線を濾紙に写し取り，その大きさに合わせて皮島をトリミングする。その露出する皮膚の位置決めは側臥位では困難であるため，仰臥位に体位を戻して左右の乳房を見比べながら再建を行った方が無難である。

いずれの再建手技においても創閉鎖後，乳房再建部と背部に陰圧吸引ドレーンを挿入して手術を終了する。

III 症　例

【症例1】右乳癌SSM後の一次再建症例（40歳）

乳房外側切開から乳輪乳頭周囲皮膚も一部含めたSSMを施行し，腋窩リンパ節はセンチネルリンパ節生検を施行した。広背筋皮弁は皮膚のしわの方向に7×17 cmの皮島をデ

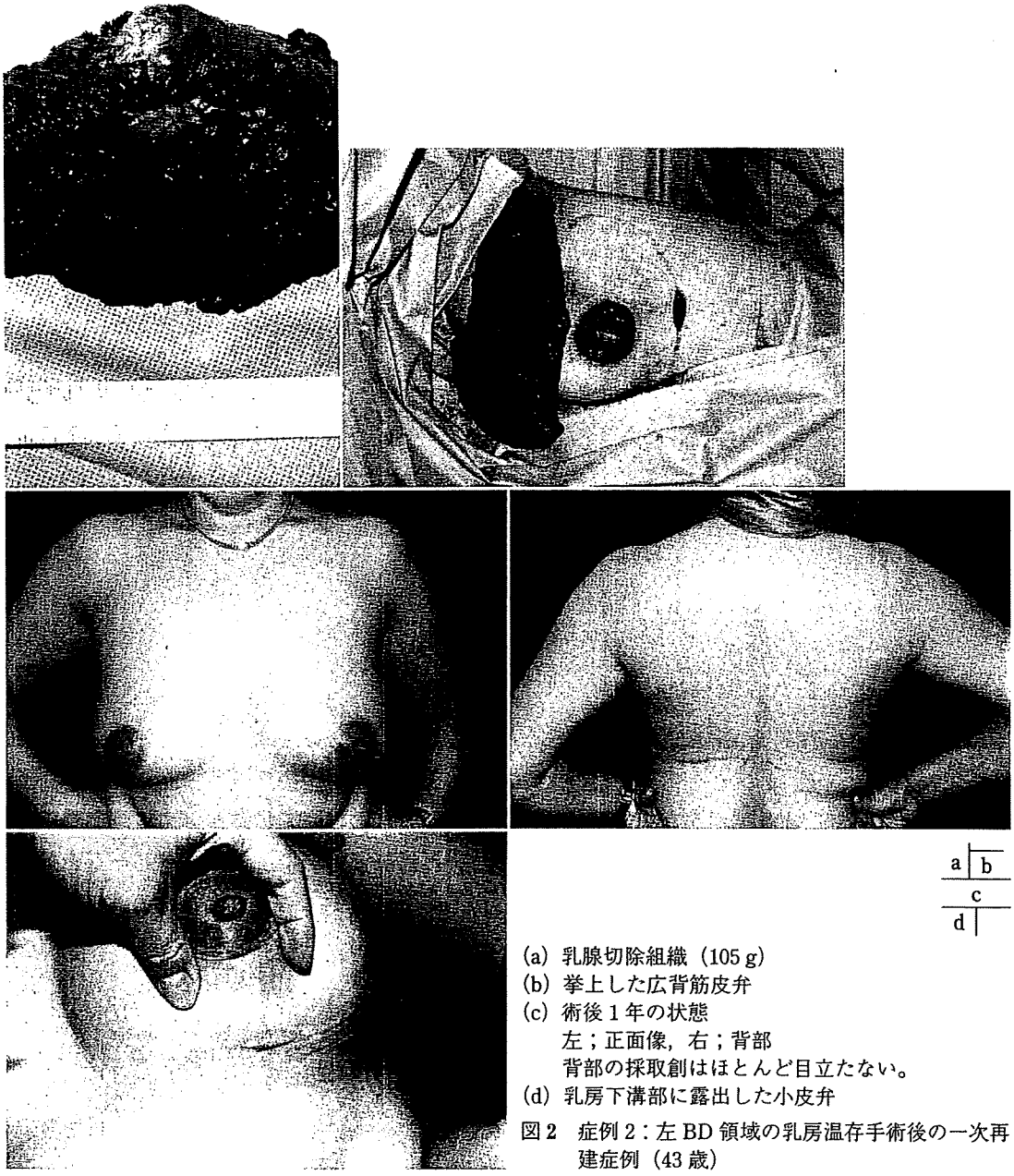

(a) 乳腺切除組織（105 g）
(b) 挙上した広背筋皮弁
(c) 術後 1 年の状態
　左；正面像，右；背部
　背部の採取創はほとんど目立たない。
(d) 乳房下溝部に露出した小皮弁

図 2　症例 2：左 BD 領域の乳房温存手術後の一次再建症例（43 歳）

ザインして大きめに採取した。皮膚欠損部に皮弁をはめ込み充填術を施行した。術後 6 カ月で，健側乳頭半切移植による乳頭再建と刺青による乳輪再建を行った。術後 1 年の状態は乳房表面の皮膚切除部に背部皮膚が露出してパッチワーク様の外観を呈しているが，乳房の大きさ・形ともほぼ対称的である。背部の採取創は斜めに瘢痕があり，やや目立つ（図 1）。

【症例 2】左 BD 領域の乳房温存手術後の一次再建症例（43 歳）

乳房外側と乳輪外側半周切開から BD 領域の乳房部分切除術（切除乳腺組織量 105 g）を施行した。腋窩リンパ節はセンチネルリン